BioEnergy Research (2024) 17:598–611
https://doi.org/10.1007/s12155-023-10636-0

Biodiesel Production from Microalgae: Exergy Analysis Using Specific Exergy Costing Approach

Eduardo J. C. Cavalcanti[1] · **Diego S. Barbosa**[1] · **Monica Carvalho**[2]

Received: 22 March 2023 / Accepted: 2 July 2023 / Published online: 14 July 2023

Abstract

Current biodiesel production research has focused on improving its energy performance and identifying and decreasing inefficiencies. To this end, exergy analysis can help develop, assess, and enhance biodiesel production plants. This study presents the exergy assessment of microalgae biodiesel production, which includes mixers, a photobioreactor (PBR), centrifuges, pumps, dryers, an extractor, tanks, heat exchangers, reactor, a washer, a distillation column, flash valve, and hydrocyclone. The first phase is algae cultivation, followed by oil extraction. The third phase is transesterification, where algal oil is separated by methane into biodiesel and glycerin. The fourth phase is biodiesel purification, followed by methanol recovery/glycerin separation. The model of the biodiesel production plant is based on mass, chemical species, energy, and exergy balances. It was verified that 93.4% of the inlet exergy originates from sunlight, with a low exergy efficiency (11.46%) obtained for the PBR. This component presented a very low energy efficiency (2.7%) and the highest destruction of exergy: 2287 GJ is destroyed, corresponding to 99.36%. The highest exergy efficiency was obtained for dryer #3 (99.99%), but other components also presented values over 99%. Finally, this study critically compares the results obtained herein with scientific literature data, highlighting data gaps and inconsistencies. The exergy assessment presented a detailed biodiesel production process from microalgae and can be used to support the improvement of production costs to motivate widespread adoption.

Keywords Bioenergy · SPECO · Exergetic efficiency · *Chlorella* microalgae · Biofuel

Introduction

The world energy matrix is predominantly fossil fuel based, with almost 85% of global energy originating from fossil fuels in 2019 [1]. The consumption of fossil fuels is associated with environmental problems such as air pollution, acid rain formation, the greenhouse effect, and climate change [2]. Diesel fuel is widely used in trucks, ships, and trains and is essential to maintain the logistics of global industrial flows.

Biodiesel is a renewable fuel with fewer environmental impacts and is an alternative to diesel. Typically, transesterification reactions are used for biodiesel production, in which an animal or vegetable oil (fat) reacts with alcohol and yields glycerol as a by-product. A catalyst is usually also present to increase the reaction rate and yield. Despite the diversity of raw materials for the production of biodiesel (e.g., animal fat, waste oil from frying, palm oil, and sunflower oil, to name a few [3]), Brazilian biodiesel production is dominated by soybean oil [4]. Because soy is a commodity, it is influenced by variations in the stock exchange market, and sometimes, biodiesel production from soybean oil is not economically advantageous. The National Biofuels Policy (RenovaBio) was launched in 2017 to support the Brazilian Nationally Determined Contribution commitments under the Paris Agreement and focuses on increasing biofuel consumption and its expansion in the Brazilian energy matrix [5]. RenovaBio included a plan to implement annual 1% increases to the country's biodiesel mixture mandate—however, supply and price concerns related to the COVID-19 pandemic forced adjustments in the original plan. Brazil's National Energy Policy Council approved an increase in the mandatory mixture of biodiesel within diesel to 13% by

✉ Eduardo J. C. Cavalcanti
eduardo.cavalcanti@ufrn.br; educanti@gmail.com

[1] Department of Mechanical Engineering, Federal University of Rio Grande Do Norte, Natal, Rio Grande do Norte 59072-970, Brazil

[2] Department of Renewable Energy Engineering, Federal University of Paraíba (UFPB), João Pessoa, Paraíba, Brazil

April 2024, reaching 14% in April 2025 and 15% in April 2026.

Algae is an excellent alternative for biodiesel production because it does not compete for land use, captures carbon dioxide (CO_2) during its production, and presents a high growth rate [6]. Algae productivity was compared by Ketheesan and Nirmalakhandan [7] in a raceway reactor, considering different CO_2 ratios of enrichment: the highest productivity was achieved at 1% CO_2 enrichment, at 0.19 dry g/(L.day).

For large-scale production, evaluating the required energy for production and seeking ways to improve its energy efficiency are essential, thus making production more financially attractive. Although the importance of energy analysis is indisputable, exergy analysis is *more* complete as it considers the irreversibilities. Exergy, unlike energy, is not conserved, so there will always be a portion of exergy that will be destroyed during a process. Exergy analysis considers the amount of energy and its quality, proving to be an essential tool in optimizing energy conversion systems [8].

In recent years, exergy assessments have been employed to improve thermodynamic processes associated with biofuels and algae growth. Ofori-Boateng et al. [9] and Sorguven and Özilgen [10] developed exergy assessments on microalgae biodiesel production, reporting significant process-related data such as masses involved, standard chemical exergy, chemical formula, and equipment configuration. However, not all data are explicit—such as information on the photobioreactor (PBR) of Ofori-Boateng et al. [9]; also, the study reported a low growth rate: the input mass of algae was 2302 kg, and after 12 days, the output was 2321.8 kg. On the contrary, most studies report higher growth rates [7, 11–14]. Chisti [15] reported that algae commonly doubles its mass after 24 h. Sorgüven and Özilgen [16] specified the inputs and outputs of the algae photosynthesis process. Ofori-Boateng et al. [17] presented a comparative exergy analysis of biodiesel production from jatropha and microalgae, presenting exergy destruction values and exergy efficiency. The authors verified that oil extraction units presented high exergy losses, and the transesterification units presented the lowest exergy losses.

Karami et al. [18] evaluated the exergy, energy, and emissions of different blends of biodiesel-diesel in a diesel engine. The biodiesel fuels were made from tomato, papaya, and apricot, and the lowest emissions were achieved by a tomato-apricot-papaya biodiesel-diesel ternary blend. The authors also reported that the maximum exergy efficiency was obtained for the tomato-papaya biodiesel blend (29.63%), while the lowest was related to pure diesel (28.46%). Hydrothermal liquefaction esterification and a conventional esterification process of microalgae for biodiesel production were compared by Prasakti et al. [19], who found similar energy results for both processes. However, the exergy assessment revealed a higher total exergy loss for the conventional transesterification process. Biodiesel production has been analyzed from an exergy viewpoint [9, 10, 17], with exergy efficiency calculated from input and output exergies. Sorgüven and Özilgen [10] focused on the transesterification and separation process and did not include algae cultivation. Although Ofori-Boateng et al. [9, 17] analyzed the entire process, some data were not explicit.

Recognizing that exergy analysis should encompass the cultivation phase (in the photobioreactor) and algae oil transesterification (in the reactor), the overarching aim of this study is to analyze biodiesel production from microalgae, encompassing all production phases. Exergy efficiencies and exergy destruction in each piece of equipment are calculated herein. The model hypothesis of algae growth for evaluation of final biomass concentration is supported by literature data. The specific chemical and physical exergies are calculated herein. Explicit data on mass increase (algae cultivation) and exergy efficiency are shown. The specific contributions of this study are (i) development of mass, energy, and exergy balances for biodiesel production; (ii) evaluation of algae growth with CO_2, H_2O, and sun energy consumption, with explicit consideration of O_2 emissions and chemical exergy; (iii) assessment of methanol recovery at distillation column, stripping, and rectifying section and flash process; (iv) calculation of global exergy efficiency and exergy destruction at each component, with the proposition of changes to improve the overall system; (v) modeling of the microalgae biodiesel plant, providing support for further feasibility studies; and (vi) identification of key components that affect global performance. The novelty is the application of the specific exergy costing (SPECO) approach within the exergy assessment, with a definition of the exergy flows of products and internal flows [20]. Data inconsistencies in scientific literature data have been identified and are discussed.

Methodology

Plant Description

The microalgae biodiesel production plant was proposed by Ofori-Boateng et al. [9, 17] to produce 1000 kg batches of biodiesel. The biodiesel plant of Ofori-Boateng et al. [9, 17] was adapted, assuming some initial data and changing some equipment, as shown in Fig. 1. The system has five phases: algae cultivation, oil extraction, transesterification, biodiesel separation, and methanol recovery.

The plant includes mixers, a photobioreactor (PBR), centrifuges, pumps, dryers, extractor, tanks, heat exchangers,

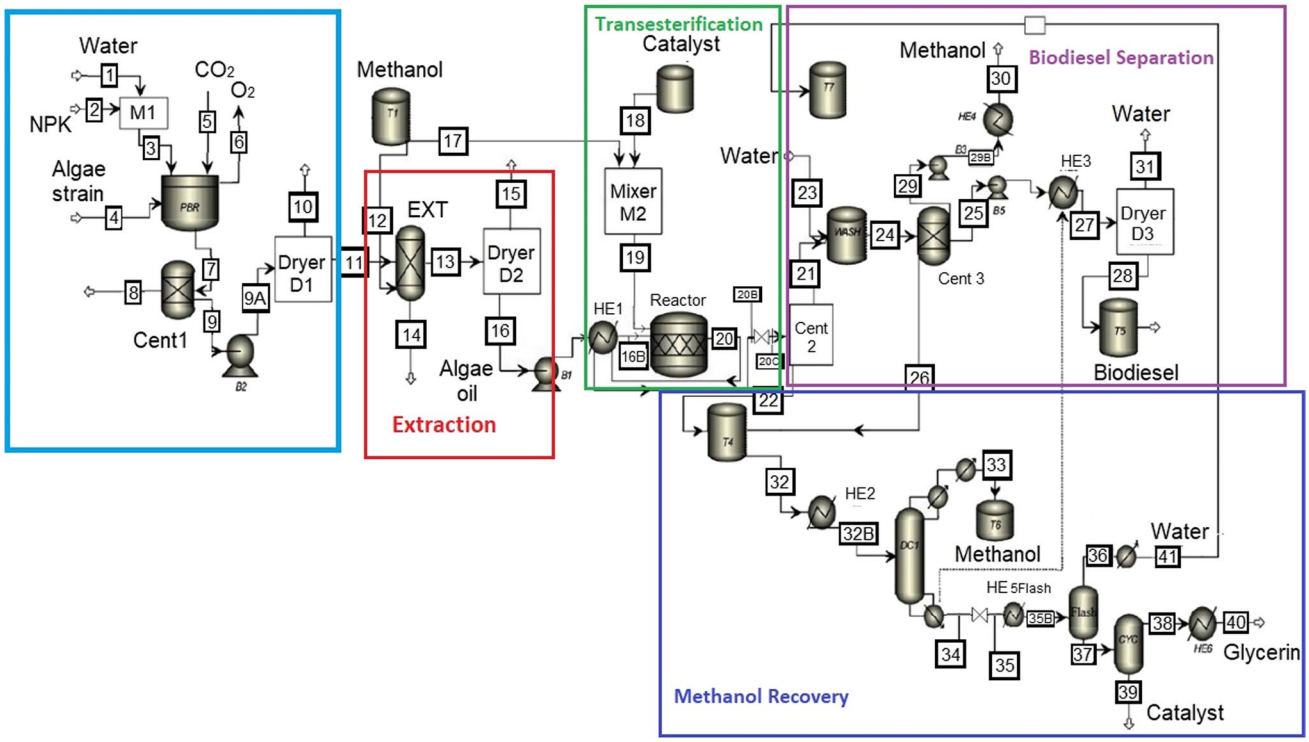

Fig. 1 Microalgae production plant

reactor, washer, distillation column, flash valve, and hydro-cyclone.

The first phase is algae cultivation. It starts with water and fertilizer being mixed. After mixing, the mixture and algae strain enter the raceway PBR and receive solar energy for 12 days to produce more algae. The temperature of the growth medium is maintained at 27 ± 1 °C. After 12 days, algae concentration has increased. The PBR raceway has 2912 m^3 water with a superficial area of 9705 m^2.

The second phase is oil extraction. Centrifuge #1 separates the excess organic medium from wet algae. The wet algae concentration follows Ofori-Boateng et al. [9]. After centrifuging, wet algae is pumped to dryer #1, which is driven by steam and yields water and dry algae.

After dryer #1, dry algae enters the extractor, where methanol is injected and algal oil is separated from the algae cake. There are many solvents available for oil extraction, such as N-hexane. Although N-hexane is more efficient in microalgae oil extraction than methanol [21], methanol is used herein, following Ofori-Boateng et al. [9], due to its lower environmental burden. Both solvents are organic substances producing respiratory damage in humans and the environmental burden of methanol is lower than that of N-hexane.

The algae cake and oil output temperatures are 55 °C [9]. Algae cake is a product of the biodiesel production plant. Algal oil and methanol enter dryer #2, where methanol is separated from the algae oil.

The third phase is the transesterification process. Algal oil is heated in heat exchanger #1 and enters the reactor with a mixture of methanol (100% excess) and a catalyst. The transesterification process is carried out at 150 °C [9], producing biodiesel and glycerin at high temperature and pressure. The output solution is cooled in heat exchanger #1, from 150 to 99.17 °C. The effectiveness of heat exchangers is 80%. The solution then flows to the expansion valve, where it reaches an environmental pressure at 64.67 °C in an isenthalpic process.

In the transesterification process, the triglyceride (algal oil) is separated by methanol into biodiesel and glycerin, following the scheme shown in Fig. 2.

In the transesterification process, triglyceride and alcohol bonds are broken. The energies of the bonds are shown for a better understanding of the broken position of chemical bond: C≡C 828 kJ/mol, C = O 724 kJ/mol, C = C 607 kJ/mol, O–H 456 kJ/mol, and C–H 410 kJ/mol [10]. The energy of the C–O bond is 358 kJ/mol, which is weak and easily broken.

The glyceride reacts with alcohol carbon producing a fatty acid methyl ester (FAME) biodiesel. The decomposed structure C_3H_5 of triglyceride reacts with the alcohol hydroxyl, forming the glycerin. Excess alcohol is used

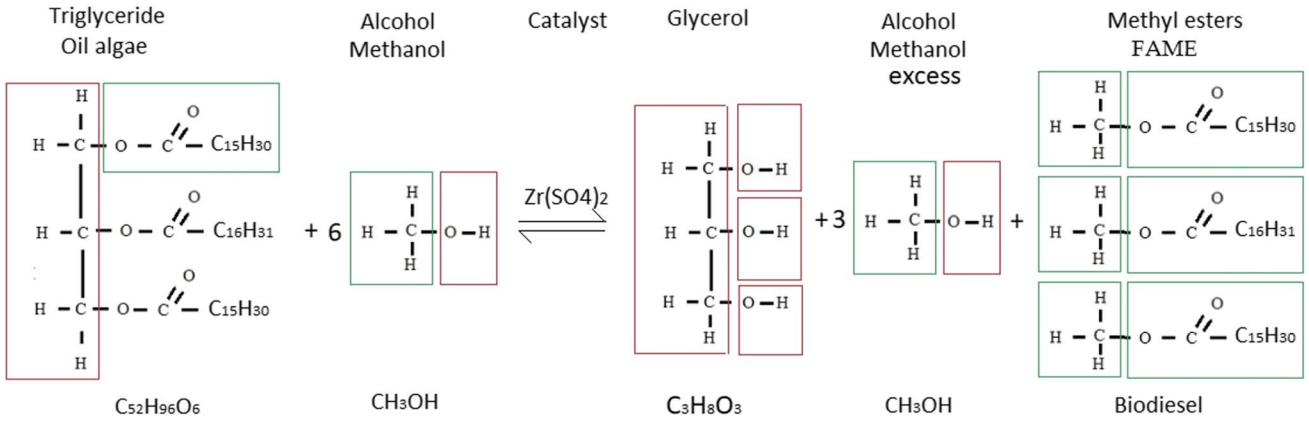

Fig. 2 Transesterification reaction: triglyceride plus alcohol in the presence of a catalyst, resulting in glycerol, methanol, and methyl ester

for transesterification to increase the reaction's efficiency, according to Ofori-Boateng et al. [9] and Sorguven and Özilgen [10]. In Ofori-Boateng et al. [9], it is stated that algal oil contains triglycerides C16:0 (palmitic acid), C18:1 (oleic acid), C18:2 (linoleic acid), C18:3 (linolenic acid), and other triglycerides in traces. In Aspen Plus software, triolein was used as the main triglyceride for the process simulation. Acid-catalyzed transesterification was employed using the solid acid catalyst sulfated zirconia (SO_4^{2-}/ZrO_2). The advantages of sulfated zirconia are the following [9]: it has the highest activity among non-sulfated heterogeneous catalysts and is a potential replacement for mineral acids like H_2SO_4, HNO_3, and HF in esterification and transesterification reactions. The solvent methanol is used at 6:1 by volume ratio. At the optimal reaction temperature of 150 °C, the overall biodiesel yield (OBY) is 98.7% of triglycerides transformed into biodiesel. The reader is directed to [9] and [10] for more details.

The fourth phase is biodiesel purification. The outputs of centrifuge #2 are two mixtures with different densities. The low-density solution (biodiesel-methanol) flows to the washer, where it is sprayed with water at 25 °C and cooled. The high-density solution (methanol–glycerin-catalyst) flows to tank #4. Centrifuge #3 generates three solutions: the first is methanol, which flows to pump #3; the second is methanol and water, which flows to tank #4; and the third is biodiesel and water, which flows to pump #5. The third solution is heated in heat exchanger #3, using the thermal energy from the column distillation boiler. Then, it enters dryer #3, where water evaporates and the product is pure biodiesel.

The fifth (and last) step is methanol recovery/glycerin separation. The mixture in tank #4 is cooled in heat exchanger #2 at 15 °C to improve the separation in the distillation column. This feed solution has a low concentration of methanol and a high amount of water. The distillation column recovers methanol at the top, using two condensers (McCabe–Thiele method), while a mixture of water, glycerin, and catalyst exits from the bottom and flows to the flash separator. The thermodynamic package and equations of state (EOS) were applied from the Engineering Equation Solver (EES software [22]). The vapor–liquid equilibrium follows Raoult's law.

Due to the high boiling point of glycerin (290 °C at atmospheric pressure), it is separated at a vacuum pressure of 10 mm Hg abs. or 1.33 kPa [23]. The advantages of vacuum distillation are reducing energy demand due to a decrease in temperature and avoiding glycerin degradation. The water vapor and the glycerin-catalyst solution are heated to 63 °C. The water steam is almost pure water, and the glycerin-catalyst mixture is separated in the hydro-cyclone.

Modeling and Assumptions

The model of the biodiesel production plant is based on mass, chemical species, energy, and exergy balances.

The PBR requirements for photosynthetic growth are sunlight, carbon dioxide, water, and inorganic salt [16]. Solar energy data was available from Natal (Northeast Brazil). The raceway PBR is 0.3 m deep [15]. CO_2 and H_2O consumptions and O_2 emissions were evaluated considering the chemical species balance for biomass production, adapted by Sorguven and Özilgen [10] and shown in Eq. 1.

$$C_{24}H_{44}O_6 + \alpha_1\left(4.17CO_2 + 0.04NH4^+\right) + \alpha_2H_2O \rightarrow \alpha_3C_{52}H_{96}O_6 + \alpha_4C_{24}H_{44}O_6 + \alpha_5O_2 \quad (1)$$

α represents the number of moles of each chemical species or the stoichiometric coefficients. The compositions of algae oil (triolein) and microalgae leftover after oil extraction are $C_{52}H_{96}O_6$ and $C_{24}H_{44}O_6$, respectively. This assumption is based on Sorguven and Özilgen [10], which considered that the algae consist of two parts: the lipids and the remainder of the cell.

The experimental characterization of algae can encompass nucleic acid, proteins, carbohydrates, and lipids in varying proportions. Lipids are extracted from the harvested algae and converted into algal oil. However, Ofori-Boateng et al. [9] and Sorguven and Özilgen [10] did not show the characterization of algae, and therefore, the present work assumed the two parts according to Sorguven and Özilgen [10].

Two chemical formulations were considered for the produced biomass, as the oil extraction phase yields algae cake and oil (and the specific exergy of cake is similar to strained algae [9]).

The production of 100 kg of algae requires 0.22 kg of $Ca(OH)_2$, 0.67 kg of KCl, 0.72 kg of $MgSO_4$, 0.85 kg of Na_2SO_4, 0.15 kg of $FeCl_2$, 10.54 kg of NH_4OH, 2.95 kg of H_3PO_4, 249.79 kg of CO_2, and 4894.84 kg of H_2O [16].

The volumetric productivity (VP) of the PBR (dry g/(L.day)) calculates the increase in biomass. The variation of input and output concentration (dry g/L) per time (day) is used according to Eq. 2.

$$\mathrm{VP} = \frac{(C_{\mathrm{out}} - C_{\mathrm{in}})}{\mathrm{time}} \tag{2}$$

The input concentration of algae strain in the raceway PBR is 0.15 g/L; after 12 days, it is 0.8 g/L [7]. This variation of biomass concentration corresponds to a volumetric productivity of 0.054 g/(L.day) in experiments with a lower CO_2 ratio of 0.035% [7]. The environmental air is assumed wet with volumetric composition of 20.59% O_2, 77.48% N_2, 1.805 H_2O, and 0.035% CO_2 [8].

The energy balance follows Eq. 3, considering a steady-state volume control.

$$\sum \dot{m}_{\mathrm{in}} h_{\mathrm{in}} - \dot{W} = \sum \dot{m}_{\mathrm{out}} h_{\mathrm{out}} + \dot{Q} \tag{3}$$

$\dot{m}$ and h are mass flow rate and specific enthalpy, respectively (kg/s and kJ/kg), $\dot{W}$ represents power, and $\dot{Q}$ represents heat rate, both in kW.

As some components operate in batches, the energy balance follows Eq. 4 for a closed system.

$${}_1Q_2 - {}_1W_2 = m_2 u_2 - m_1 u_1 \tag{4}$$

Q_2 and ${}_1W_2$ refer to the heat and work from state 1 to 2, respectively (kJ), m is mass (kg), and u is the specific internal energy (kJ/kg).

When there is a chemical reaction in a piece of equipment, such as in the raceway PBR and transesterification reactor, the enthalpy of formation must be adopted in the energy balance. It is necessary to evaluate the higher heating value (HHV) to calculate the formation enthalpy of oil algae and biodiesel, as given by Eq. 5, according to Miao et al. [24].

$$\mathrm{HHV} = 0.3383\mathrm{C} + 1422\left(\mathrm{H} - \frac{\mathrm{O}}{8}\right) \tag{5}$$

$$\sum_F n \times \overline{h_F} + \mathrm{HHV} \times M = \sum_P n \times \overline{h_f} \tag{6}$$

C, H, and O are the carbon, hydrogen, and oxygen mass percentages. n is the number of moles, $\overline{h_F}$ is the enthalpy of formation, and M is the molecular mass of fuel. Subscripts F and P refer to fuel and product, respectively.

The following assumptions were made to model the biodiesel production plant:

- The work of mixers #1 and #2 is 57.45 MJ and 22.00 MJ, respectively [17].
- The mass of NPK fertilizer mass is 304.7 kg [16]. The work of centrifuge #1 is 12,785.73 MJ, proportional to Ofori-Boateng et al. [9], which uses 4.39 kJ per kg of solution.
- The energy efficiency of dryer #1 is 90%, according to [25]. The steam temperature is 110 °C to evaporate water with an assumed temperature gradient of 10 °C. Such a low-temperature gradient is used to maintain high efficiency.
- The energy efficiency of the extractor is 99%. The steam temperature of dryer #2 is 100 °C to evaporate methanol, corresponding to the saturation temperature for atmospheric pressure, with an energy efficiency of 95%.
- The energy efficiency of the reactor is 90%, according to [25], with 160 °C steam temperature and an assumed temperature gradient of 10 °C. The energy required to mix the solution is 41 MJ [9].
- The efficiencies of dryers and reactor were considered different because of the mass, temperature, and fluid to evaporate.
- All heat exchangers have an effectiveness of 80% [25].
- In centrifuge #2, the work consumed is 48 MJ [9]; in the washer, the work consumed was 16 MJ [9], and it was considered that 20% of this work is converted to thermal energy.
- In dryer #3, the steam temperature for evaporation is 110 °C with an assumed temperature gradient of 10 °C.
- Heat exchanger #2 uses chilled water at 8 °C to cool the input solution of the distillation column.
- Flash heat exchanger #5 uses steam at 100 °C, corresponding to the saturation temperature for atmospheric pressure to heat the mixture to 63 °C.
- In the hydro-cyclone and all centrifuges, 20% of the work is converted into thermal energy, and the remainder produces the kinetic energy of the solution.

Table 1 Enthalpy of formation, specific heat capacity, and standard chemical exergy of chemical species

Species	$\overline{h_f}$(kJ/kg)	cp (kJ/kg)	e^0_{CH}(kJ/kg)
Biodiesel ($C_{18}H_{34}O_2$)[a]	Calculated	2.64[b]	Calculated
Algal oil ($C_{52}H_{96}O_2$)[a]	Calculated	2.66[b]	Calculated
Algae strain ($C_{24}H_{44}O_6$)[a]	Calculated	4.19[i]	64,200.0[a]
Methanol (CH_3OH)g	− 6282[e]	1.38[d]	22,542.0[h]
Methanol (CH_3OH)l	− 7466[e]	2.53[d]	22,408.0[h]
Glycerin ($C_3H_8O_3$)	− 7275[c]	2.39[c]	22,952.0[c]
Catalyst ($Zr(SO_4)_2$)	–	0.61[d]	–
Water (H_2O)g	− 13,423[e]	1.87[d]	527.3[h]
Water (H_2O)l	− 15,865[e]	4.18[d]	49.9[h]
NH_4OH	− 10,466[f]	4.42[d]	9384.0[g]
H_3PO_4	− 13,110[d]	1.08[d]	822.5[g]
Na_2SO_4	− 9766[d]	0.90[d]	134.8[g]
KCl	− 5855[d]	0.05[d]	189.9[g]
$MgSO_4$	− 10,680[d]	0.80[d]	271.4[g]
$Ca(OH)_2$	− 13,300[d]	1.18[d]	1395[g]
$FeCl_2$	− 2697[d]	0.60[d]	1259[g]

[a][17]
[b][10] adapted
[c][10]
[d][26]
[e][27]
[f][28]
[g][16]
[h][8]
[i][29]

Table 1 shows the parameters employed to carry out the simulations.

Exergy Analysis

Exergy rates can include physical, chemical, potential, and kinetic shares. Potential and kinetic exergy shares are considered negligible. Physical (e^{PH}) and chemical (e^{CH}) exergies are evaluated by Eqs. 7 and 8.

$$e^{PH} = (h - h_0) - T_0(s - s_0) \tag{7}$$

$$e^{CH} = \sum y_i e^0_{CH} + RT_0 \sum y_i \ln(y_i) \tag{8}$$

h is the specific enthalpy (kJ/kg), T is the temperature (K), s is the specific entropy (kJ/kg.K); e^0_{CH} is the standard chemical exergy of each chemical species, R is the universal gas constant, and y_i represents the molar fraction of each chemical species. However, some components operate in batches (e.g., dryer) and follow Eq. 9.

$$e^{Ph} = (u - u_0) - T_0(s_0 - s_0) + P_0(v - v_0) \tag{9}$$

u is the specific internal energy (kJ/kg) and v is the specific volume (m^3/kg).

Following the SPECO approach, fuel and product exergies are defined in the productive structure, following Eq. 10.

$$E_F = E_P + E_D \tag{10}$$

E_F is the fuel exergy, E_P is the product exergy, and E_D is destroyed exergy. The fuel exergy is all exergy decreases between inlet and output streams and all inlet exergy. Fuel exergy encompasses the resources expended to achieve a result. The product exergy is all increase of exergy between inlet and outlet streams plus all output exergy that are in accordance with the purpose of the equipment. The SPECO approach separates the physical and chemical exergy into product or fuel, depending on the definition of the device.

The exergy efficiencies (ε) can be calculated with Eq. 11.

$$\varepsilon = \frac{E_P}{E_F} \tag{11}$$

The exergy rates of fuel and product for each component are shown in Table 2, based on the SPECO approach.

The exergy rate of the Sun at the PBR raceway is evaluated according to Petela [30], where the Sun's temperature is 5770 K.

Mass, chemical species, energy, and exergy balances were modeled and calculated with EES [22].

Results and Discussions

Mass and Species Chemical Balances

The algae cultivation phase is designed to produce 1000 kg of biodiesel. The input concentration is 0.15 g/L, and after 12 days, algae concentration reaches 0.8 g/L, yielding a PBR volumetric productivity of 0.05417 dry g/(L.day) calculated by Eq. 2. This results in dry algae production of 1892 kg. A similar initial concentration of strain in the PBR raceway is found in Ketheesan and Nirmalakhandan [7] and Morais and Costa [14]. Other works used a slighter lower value, such as 0.01 g/L in Ryu et al. [13] and 0.035–0.04 g/L in Mtaki et al. [15, 16]. Ofori-Boateng et al. [9] reported an initial algae concentration of 0.02 g/L (no explicit data were included); however, mass balance calculations lead to a much higher value (2302.1/11,529 × 1000 g/1 kg = 199.7 g/L). The production of algae was only 20 kg, which seems inconsistent and does not follow literature trends [7, 11–14]. The output concentration of dry algae is within the scientific

Table 2 Definition of the exergy rate of fuels and products for each component

Equipment	EF	EP
Mixer 1	$\left(e_2^T - e_3^T\right)m_2 - W_{\text{mixer1}}$	$\left(e_3^T - e_1^T\right)m_1$
PBR raceway	$E_3 + E_4 + E_5 + E_{\text{Sun}} - W_{\text{PBR}}$ $E_{\text{Sun}} = Q\left(1 - \frac{4}{3}\frac{T_0}{T_s} + \frac{1}{3}\frac{T_0}{T_s^4}\right)$	$E_6 + E_7$
Centrifuge 1	$\left(e_7^{\text{ch}} - e_8^{\text{ch}}\right)m_8 - W_{\text{cent1}}$	$\left(e_9^T - e_7^T\right)m_9 + \left(e_8^{\text{ph}} - e_7^{\text{ph}}\right)m_8$
Dryer 1	$\left(e_9^{\text{ch}} - e_{10}^{\text{ch}}\right)m_{10} + Q_{\text{Dry1}}\left(1 - \frac{298}{\text{TK}_{\text{stDRy1}}}\right)$	$\left(e_{11}^T - e_9^T\right)m_{11} + \left(e_{10}^{\text{ph}} - e_9^{\text{ph}}\right)m_{10}$
Extractor 1	$\left(e_{11}^T - e_{13}^T\right)m_{13\text{oil}} + \left(e_{11}^T - e_{14}^T\right)m_{14\text{algae}} - W_{\text{ext}}$	$\left(e_{13}^T - e_{12}^T\right)m_{13\text{met}} + \left(e_{14}^T - e_{12}^T\right)m_{14\text{met}}$
Dryer 2	$\left(e_{13}^{\text{ch}} - e_{15}^{\text{ch}}\right)m_{15} + Q_{\text{Dry2}}\left(1 - \frac{298}{\text{TK}_{\text{stDRy2}}}\right)$	$\left(e_{16}^T - e_{13}^T\right)m_{16} + \left(e_{15}^{\text{ph}} - e_{13}^{\text{ph}}\right)m_{15}$
Heat exchanger 1	$\left(e_{20}^T - e_{20b}^T\right)m_{20}$	$\left(e_{16b}^T - e_{16}^T\right)m_{16}$
Mixer 2	$\left(e_{17}^{\text{ch}} - e_{19}^{\text{ch}}\right)m_{17} - W_{\text{mix2}}$	$\left(e_{19}^T - e_{18}^T\right)m_{18} + \left(e_{19}^{\text{ph}} - e_{17}^{\text{ph}}\right)m_{17}$
Reactor	$\left(e_{16}^{\text{ch}} - e_{20}^{\text{ch}}\right)m_{16} - W_R + \frac{Q_R}{\eta_R}\left(1 - \frac{298}{\text{TK}_{\text{stR}}}\right)$	$\left(e_{20}^T - e_{19}^T\right)m_{19} + \left(e_{20}^{\text{ph}} - e_{16b}^{\text{ph}}\right)m_{16}$
Centrifuge 2	$\left(e_{20}^{\text{ch}} - e_{22}^{\text{ch}}\right)m_{22} + \left(e_{20c}^{\text{ph}} - e_{22}^{\text{ph}}\right)m_{22} - W_{\text{Cent2}}$	$\left(e_{21}^{\text{ch}} - e_{20}^{\text{ch}}\right)m_{21} + \left(e_{21}^{\text{ph}} - e_{20c}^{\text{ph}}\right)m_{21}$
Washer	$\left(e_{21}^T - e_{24}^T\right)m_{21} - W_{\text{Wash}}$	$\left(e_{24}^T - e_{23}^T\right)m_{23}$
Centrifuge 3	$\left(e_{24}^{\text{ch}} - e_{26}^{\text{ch}}\right)m_{26} + \left(e_{24}^{\text{ph}} - e_{29}^{\text{ph}}\right)m_{29}$ $+\left(e_{24}^{\text{ph}} - e_{25}^{\text{ph}}\right)m_{25} - W_{\text{Cent3}}$	$\left(e_{26}^{\text{ph}} - e_{24}^{\text{ph}}\right)m_{26} + \left(e_{29}^{\text{ch}} - e_{24}^{\text{ch}}\right)m_{29}$ $+\left(e_{25}^{\text{ch}} - e_{24}^{\text{ch}}\right)m_{25}$
Heat exchanger 3	$E_{\text{stHE3}} - E_{\text{stHE3b}}$	$E_{27} - E_{25}$
Dryer 3	$\left(e_{27}^{\text{ch}} - e_{31}^{\text{ch}}\right)m_{31} + Q_{\text{Dry3}}\left(1 - \frac{298}{\text{TK}_{\text{stDRy3}}}\right)$	$\left(e_{28}^T - e_{27}^T\right)m_{28} + \left(e_{31}^{\text{ph}} - e_{27}^{\text{ph}}\right)m_{31}$
Tank T4	$\left(e_{26}^{\text{ph}} - e_{32}^{\text{ph}}\right)m_{26} + \left(e_{22}^{\text{ch}} - e_{32}^{\text{ch}}\right)m_{22}$	$\left(e_{32}^{\text{ph}} - e_{22}^{\text{ph}}\right)m_{22} + \left(e_{32}^{\text{ch}} - e_{26}^{\text{ch}}\right)m_{26}$
HE2	$E_{\text{stHE2}} + E_{32}$	$E_{\text{stHE2b}} + E_{32}$
Distillation Column	$\left(e_{32}^{\text{ch}} - e_{34}^{\text{ch}}\right)m_{34} + E_{\text{boi}} - \left(E_{\text{cond1}} + E_{\text{cond2}}\right)$	$\left(e_{34}^{\text{ph}} - e_{32}^{\text{ph}}\right)m_{34} + \left(e_{33}^T - e_{32}^T\right)m_{33}$
Flash 1	$\left(e_{34}^{\text{ph}} - e_{37}^{\text{ph}}\right)m_{37} + \left(e_{34}^T - e_{36}^T\right)m_{36} + E_{\text{HEflash}}$	$\left(e_{37}^{\text{ch}} - e_{34}^{\text{ch}}\right)m_{37}$
Hydro-cyclone	$\left(e_{37}^{\text{ch}} - e_{39}^{\text{ch}}\right)m_{39} + W_{cic}$	$\left(e_{38}^T - e_{37}^T\right)m_{38} + \left(e_{39}^{\text{ph}} - e_{37}^{\text{ch}}\right)m_{39}$

literature range: 0.4–4.1 g/L after 20 days by Morais and Costa [14], 0.8–1.3 g/L by Ketheesan and Nirmalakhandan [9], and 0.4–1.9 by Mtaki et al. [15, 16]. Ryu et al. [13] reached 1.1–2 g/L operating with 6 days. This higher value was achieved due to the aeration of gas, with CO_2 content between 0.5% and 5.0%, while the present work was modeled with a CO_2 content of 0.035%.

Considering the photosynthesis reaction (Eq. 1), the stoichiometric coefficients are (α_1) 111 kmol of CO_2, (α_2) 102.1 kmol of H_2O, (α_3) 1.115 kmol of algae oil, (α_4) 3.207 kmol of biomass (strain and cake), and (α_5) 152 kmol of O_2.

As the intended production is 1000 kg of biodiesel, so 1.019 kmol of strain is necessary (Eq. 1). All stoichiometric coefficients (α_s) are multiplied by 1.019, resulting in the capture of 5077 kg CO_2 from the environment and 5058 kg O_2 produced at points 5 and 6, respectively. This result is similar to Sorguven and Özilgen [16], which used 100 kg of algae (oil algae chemical formula $C_{69}H_{98}O_6$), captured 249.79 kg CO_2, and released 249.23 kg O_2. It is important to note that herein 1000 kg of biodiesel is obtained after algae oil production, considering oil algae as $C_{52}H_{96}O_6$ in Eq. 1.

Table 3 Formation enthalpies and chemical exergies of biodiesel, algal oil, and algae strain

Chemical species	h_F(kJ/kg)	h_F(MJ/kmol)	e^{ch}(kJ/kg)	e^{ch}(MJ/kmol)
Biodiesel ($C_{18}H_{34}O_2$)	− 1080	− 295.5	39100	10702
Algal oil ($C_{52}H_{96}O_6$)	− 1518	− 1241.0	40100	32774
Algae strain ($C_{24}H_{44}O_6$)	− 1001	− 429.0	Ref. [17]	Ref. [17]

Energy and Exergy Balances

Table 3 shows the enthalpies of formation and chemical exergy values of biodiesel, algal oil, and algae strain.

The formation enthalpy and chemical exergy of biodiesel are similar to those of Sorguven and Özilgen [10], which are − 429.0 MJ/kmol and 14,299 MJ/kmol with $C_{24}H_{36}O_2$. A higher carbon content C_{24} leads to a lower formation enthalpy (negative) and higher chemical exergy in relation to the value of the present work C_{18}.

The formation enthalpy and chemical exergy of algae oil also agree with Sorguven and Özilgen [10], which presented algae oil as $C_{69}H_{98}O_6$ and values of − 1056 MJ/kmol and 40,542 MJ/kmol for formation enthalpy and chemical exergy. The difference in formation enthalpy is due to the higher heat value (HHV) used in Eqs. 5 and 6. Sorguven and Özilgen [10] did not mention the value of HHV used to calculate its formation enthalpy.

The formation enthalpy of algae strain was obtained based on its chemical exergy.

Table 4 Thermodynamic properties at each point of the biodiesel production process

Point	*m* (kg)	*T* (°C)	*P* (kPa)	e^{ph}(kJ/kg)	e^{ch}(kJ/kg)	e^{T}(kJ/kg)	*E* (GJ)
1	2,911,600.0	25.00	101.30	0.00	49.96	49.96	145.46
2	304.7	25.00	101.30	0.00	6351.54	6351.54	1.94
3	2,911,904.7	25.00	101.30	0.00	50.55	50.55	147.20
4	436.7	25.00	101.30	0.00	64,200.00	32,845.00	14.34
5	4977.2	25.00	101.30	0.00	451.49	451.49	2.25
6	4958.4	27.00	101.30	0.01	124.07	124.07	0.62
7	2,912,359.5	27.00	101.30	0.03	79.04	79.07	230.28
8	2,908,880.4	27.21	101.30	0.03	50.63	50.67	147.39
9	3479.1	27.21	101.30	0.03	23,859.16	23,859.19	83.01
10	1157.3	99.97	101.30	487.35	49.96	537.31	0.62
11	2321.8	99.97	101.30	28.93	35,744.26	35,773.19	83.06
12	6965.4	25.00	101.30	0.00	22,407.98	22,407.98	156.08
13	6849.4	55.00	101.30	3.81	24,804.31	24,808.12	169.92
14	2437.8	55.00	101.30	5.02	28,361.21	28,366.22	69.15
15	5920.7	64.87	101.30	134.66	22,407.98	22,542.64	133.47
16	928.7	64.87	101.30	6.53	40,100.00	40,106.53	37.25
17	328.5	25.00	101.30	0.00	22,407.98	22,407.98	7.36
18	70.8	25.00	101.30	0.00	0.00	0.00	0.00
19	399.3	30.00	101.30	0.10	18,427.48	18,427.58	7.36
20	1328.0	150.00	1399.78	53.59	33,804.41	33,858.01	44.96
21	1141.6	64.67	101.30	19.48	37,020.91	37,040.38	42.29
22	186.4	64.67	101.30	4.26	14,143.06	14,147.32	2.64
23	1246.4	25.00	101.30	0.00	49.96	49.96	0.06
24	2388.0	56.40	101.30	5.36	17,697.94	17,703.30	42.28
25	1124.6	57.47	101.30	4.64	34,759.06	34,763.70	39.10
26	1235.5	57.47	101.30	6.73	2082.50	2089.23	2.58
27	1124.6	97.01	101.30	21.11	34,759.06	34,780.17	39.11
28	1000.0	100.00	101.30	21.36	39,100.00	39,121.36	39.12
29	27.9	57.47	101.30	4.43	22,407.98	22,412.40	0.63
30	27.9	57.47	101.30	4.43	22,407.98	22,412.40	0.63
31	124.6	100.00	101.30	485.63	49.96	535.59	0.07
32	1421.9	57.91	101.30	6.39	3651.38	3657.78	5.20
33	136.2	65.00	101.30	134.72	22,407.98	22,542.70	3.07
34	1285.7	99.52	101.30	31.07	1692.44	1723.51	2.22
35	1285.7	11.74	1.33	1.19	1692.44	1692.13	2.17
36	1121.8	63.00	1.33	− 114.99	49.96	− 65.03	− 0.07
37	163.9	63.00	1.33	3.62	13,027.81	13,031.43	2.14
38	93.1	78.83	1.33	10.38	22,951.81	22,962.19	2.14
39	70.8	78.83	1.33	2.64	0.00	2.64	0.00

Table 4 shows the mass, temperature, pressure, physical and chemical specific exergies, specific total exergy, and exergy at each point of the biodiesel production process.

The products are biodiesel at #28 and glycerin at #38.

The specific physical exergy of water is 0.00 at point 1, and the specific physical exergy of methanol is 0.00 at point 17, both in kJ/kg and 25 °C and atmospheric pressure. In Ofori-Boateng et al. [9], the values at these points are 0.076 MJ/kg and 5.205 MJ/kg, respectively. For the water states, its temperature is 100 °C with a quality of 0.09292. For the methanol state, its temperature did not converge at a range from 175.6 to 570 K. These values of specific physical exergy are inconsistent.

In general, the pressure is the same as the environment. The transesterification process uses a metallic catalyst in the reactor, and high pressure is desired. The pressure of 1.399 MPa at #20 is used to avoid alcohol evaporation, and an expansion valve reduces the pressure to atmospheric conditions. In flash distillation, the water and glycerin are separated at vacuum conditions.

The specific physical exergy depends on temperature and pressure. The water at #36 is at vacuum pressure (1.33 kPa), and this condition produces a negative value of physical exergy due to its higher specific entropy. From Eq. 7, − 114.99 kJ/kg. A similar behavior occurred in Cavalcanti et al. [31], where the low pressure increases the entropy of water in the gaseous phase.

The chemical exergy of each component of the mixture influences the overall specific chemical exergy. The highest specific chemical exergy occurs at #16 for algae oil, and the chemical exergy of the catalyst at #18 is null. The chemical exergy is used when there is a change of composition, such as in combustion: a fuel is converted into gases of combustion products. Nonetheless, the catalyst used its structure or surface to favor the chemical reaction, and its chemical composition is the same. Therefore, its chemical exergy is null.

Figure 3 shows the exergy efficiency of each piece of equipment, and Table 5 shows the destroyed exergy and the breakdown of individual contributions to overall exergy destruction for each piece of equipment.

The equipment with the lowest energy efficiency is the PBR raceway: only 2.7%, because most energy is reflected and spread in the water, and the PBR is not designed to stock exergy. The exergy efficiency is higher (11.46%) than its energy efficiency. The solar irradiance temperature is reduced from 5770 K to the environmental temperature, reducing efficiency. A similar result was found by Sorguven and Özilgen [16], where 94.8% of exergy was destroyed during photosynthesis. The authors investigated the thermodynamic efficiency of glucose and lipid synthesis and

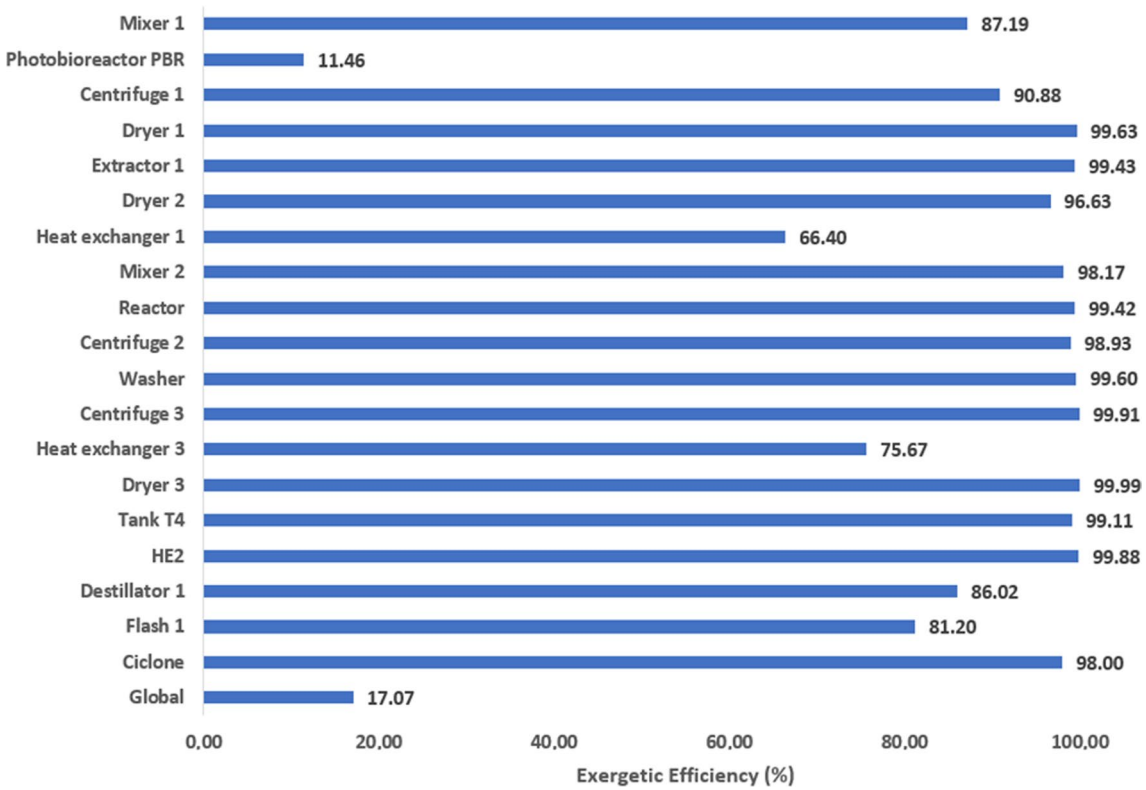

Fig. 3 Exergy efficiency per component of the biodiesel product process

Table 5 Exergy destruction and breakdown of individual contributions to overall exergy destruction

Equipment	E_D (MJ)	$\%E_D$
Mixer #1	253.28	0.01184
PBR raceway	2,123,660.59	99.30009
Centrifuge #1	12,680.00	0.59306
Dryer #1	159.92	0.00748
Extractor #1	225.08	0.01052
Dryer #2	522.97	0.02445
HE #1	14.79	0.00069
Mixer #2	24.36	0.00114
Reactor	35.76	0.00167
Centrifuge #2	39.71	0.00186
Washer	88.10	0.00412
Centrifuge #3	17.67	0.00083
HE #3	5.96	0.00028
Dryer #3	0.45	0.00002
Tank #4	17.32	0.00081
HE #2	6.30	0.00029
Distillation column	424.62	0.01985
Flash	430.08	0.02011
Cyclone	18.88	0.00088

breakdown by photosynthetic microalgae, concluding that 99.6% of the inlet exergy comes from sunlight and its exergy efficiency is 4.93% (percentage of inlet exergy converted into biomass). Herein, 93.4% of the inlet exergy comes from sunlight, and the exergy efficiency is higher (11.46%). The lower exergy efficiency obtained by [18] was a result of considering many metabolic pathways, such as the storage of inlet exergy in the algal lipid, conversion of glucose into lipid, photosynthetic glucose production by microalgae, reconversion of storage lipids into glucose, production of glycogen for storage, and reconversion of glycogen into glucose. As more pathways are included, this lowers the exergy efficiency. The inputs of CO_2, H_2O, strains, and solar energy with O_2 emissions were considered herein and in [18]. Castiñeiras-Filho and Pradelle [32] obtained a 99.47% exergy efficiency for microalgae cultivation; however, there was no further information on the solar exergy rate (which is very relevant to microalgae growth). The PBR raceway presents the highest destruction of exergy: the sun provides 2379.0 GJ exergy, and 274.5 GJ is converted into the product (2287 GJ is destroyed, 99.36%). In Ofori-Boateng et al. [9], exergy destruction is 566 MJ, significantly lower than herein—however, data on masses and solar irradiance were not explicit.

Observing other components, the highest exergy efficiency was obtained at dryer #3, but other components also presented values over 99% (dryer #1, oil extractor, reactor, washer, centrifuge #3, tank #4, and heat exchanger #2). Similar results were obtained by Castiñeiras-Filho and Pradelle [32], who modeled biodiesel production from microalgae integrated into a sugarcane ethanol plant. Many of the components presented exergy efficiencies higher than 90%, and the biomass drying reached an exergy efficiency of 98.5%. Peralta-Ruiz et al. [21] obtained a lower exergy efficiency when using hexane and methanol–chloroform in the oil extractor: 50% and 30%, respectively. The difference is because Peralta-Ruiz et al. [21] modeled the microalgae composition using many components, such as free fatty acids, triglycerides, amino acids, carbohydrates, and water. Herein, algae were assumed to consist of lipids and the rest of the cell [10].

The lowest exergy destruction was obtained at dryer #3—although this device evaporates water, its initial temperature is already high, and therefore, dryer #3 uses a small quantity of exergy. In mixer #1, 138,4 MJ of exergy was destroyed. Although a higher mass was considered herein, Ofori-Boateng et al. [17] reported 171 MJ exergy destroyed. Centrifuge #1 presented an exergy efficiency of 90.88%, the second component with the highest exergy destruction. In Ofori-Boateng et al. [9], this centrifuge destroyed 925 MJ; in this paper, exergy destruction is 12,680 MJ (due to higher water mass flow rate).

In dryer #1, Ofori-Boateng et al. [9] used 167 MJ to evaporate water. However, calculations revealed that the energy required should be 3746 MJ, with a 90% energy efficiency. The exergy destruction calculated by SPECO is 159.94 MJ, much lower than the 787 MJ obtained by Ofori-Boateng et al. [9]. The oil extractor destroys 225.09 MJ of exergy against 158 MJ reported by Ofori-Boateng et al. [9].

In dryer #2, the energy required to evaporate methanol was calculated (6224 MJ), assuming 95% energy efficiency, leading to an exergy destruction of 522.97 MJ. In Ofori-Boateng et al. [9], dryer #2 destroyed 887 MJ exergy. As the output temperature of the reactor is high (150 °C), a heat exchanger was included to harness thermal energy to heat the algal oil before the reactor. Heat exchanger #1 increases the algal oil temperature from 64.87 to 127 °C and decreases the output reactor flow to 99.25 °C. Heat exchanger #1 presented an exergy destruction of 10.93 MJ with 75.13% exergy efficiency. Mixer #3 presents an exergy destruction of 24.89 MJ, similar to Ofori-Boateng et al. [9] (23 MJ).

During transesterification, the energy demand calculated by the first law of thermodynamics is 947 MJ for the reactor. The reactor pressure is 1400 kPa to ensure that all fluids are liquid and that methanol does not evaporate at 150 °C. The exergy efficiency of the transesterification reactor is 99.42%, with an exergy destruction of 35.76 MJ. The transesterification phase includes the reactor, dryer #2, centrifuge #2, washer, centrifuge #3, and dryer #3 [11]. Exergy destruction and exergy efficiency were calculated

by input and output exergies. These values are 430.39 MJ with 85.61% herein, respectively. Although Ofori-Boateng et al. [9] used a different chemical composition of algae oil, alcohol, and biodiesel, its values were similar, 629 MJ and 82.89%. The transesterification phase presented a better performance herein due to the addition of heat exchanger #1, which reduced the energy consumed. Castiñeiras-Filho and Pradelle [32] reached a lower exergy efficiency (77%) in the transesterification reactor, due to the utilization of sugarcane bagasse instead of microalgae.

Regarding centrifuge #2 in the biodiesel purification phase, this component presented high exergy efficiency and 39.71 MJ of exergy destruction. Exergy destruction in the centrifuge of Ofori-Boateng et al. [9] was 255 MJ. Ofori-Boateng et al. [9] explained that this exergy destruction is due to the composition or quality of the resource input to the centrifuge.

The washer used water at 25 °C, and its exergy destruction is 88.10 MJ, while Ofori-Boateng et al. [9] used water at 55 °C and reported 64 MJ of exergy destroyed. The input of the washer includes gaseous methanol that should be condensed. The water temperature is herein selected at environmental conditions to avoid environmental issues associated with methanol leakage.

In centrifuge #3, methanol, glycerin, and water are separated from biodiesel. The exergy destruction was 17.67 MJ, while Ofori-Boateng et al. [9] reported 151 MJ. As mentioned by Kim et al. [33], centrifugation is more effective for a fast separation but is not cost-effective for the mass production of lipids [9]. After centrifuge #3, a heat exchanger integrated with a distillation column boiler was used, with 7.29 MJ exergy destruction. Dryer #3 evaporates water and requires 270 MJ energy, with 1.03 MJ exergy destruction against 140 MJ of Ofori-Boateng et al. [9].

In the distillation column, the molar concentrations of feed, methanol (at the column's top), and water (at the column's bottom) are 5.17%, 97.00%, and 0.16%, respectively. For this condition, the feed mixture temperature is 15 °C, due to the low feed methanol concentration. Heat exchanger #2 supplies this temperature using 1365 kg of chilled water at 8 °C and destroying 6.69 MJ exergy. The distillation column boiler operates with 785 kg of steam (110 °C), and the two condensers operate with water at 25 °C, using 8900 kg and 1165 kg of water, respectively. Figure 4 shows the graph of the McCabe–Thiele method, which displays the feed line (gray), the rectification line (yellow), the curve (dark blue), the stripping line (light blue), and all steps of the method.

The distillation column has 11 ideal stages, two condensers, and a reflux ratio of 7.5. The distillation column achieved an exergy efficiency of 87.75% with 432.84 MJ exergy destruction. The distillation column of

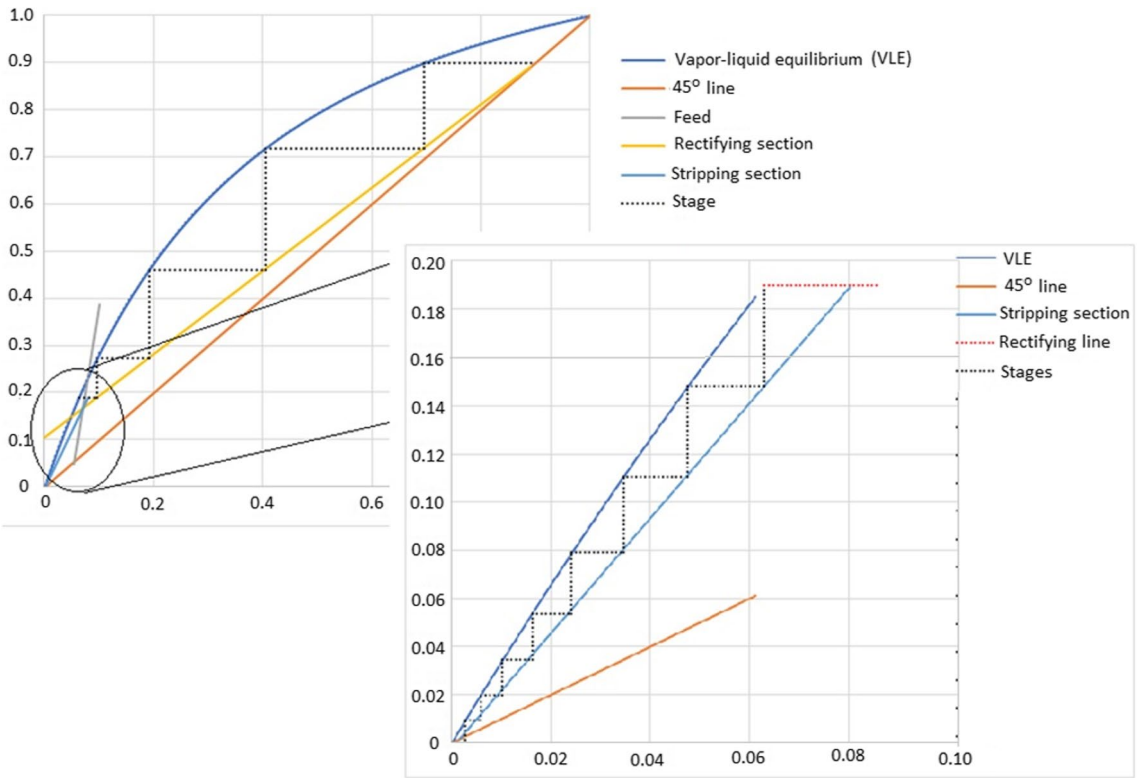

Fig. 4 McCabe–Thiele method to model the separation of substances by a distillation column

Table 6 Comparison of results with scientific literature data

Parameters	Present work	Value	References
Initial dry density of algae culture (g/L)	0.15	199.67	Ofori-Boateng et al. [9, 17]
		0.01	Ryu et al. [11]
		0.15	Morais and Costa [12]
		0.15	Ketheesan and Nirmalakhandan [7]
		0.035–0.04	Mtaki et al. [13, 14]
Final dry density of biomass (g/L)	0.80 (12 days)	201.38 (12 days)	Ofori-Boateng et al. [9, 17]
		1.1–2 (6 days)	Ryu et al. [11]
		0.4–4.1 (20 days)	Morais and Costa [12]
		0.8–1.3 (12 days)	Ketheesan and Nirmalakhandan [7]
		0.4–1.9 (12 days)	Mtaki et al. [13, 14]
Dry algae mass produced (kg)	1892	19.7	Ofori-Boateng et al. [9, 17]
Water physical exergy (kJ/kg)	0.0 at point 1 (25 °C)	76.0 unknown condition	Ofori-Boateng et al. [9, 17]
Methanol physical exergy (kJ/kg)	0.0 at point 17 (25 °C)	5,205 unknown condition	Ofori-Boateng et al. [9, 17]
Exergetic efficiency of cultivation unit	11.46%	4.93%	Sorguven and Özilgen [16]
		99.47%	Castiñeiras-Filho and Pradelle [32]
		99.47%	Ofori-Boateng et al. [9, 17]
Exergetic efficiency of transesterification unit	85.61%	82.89%	Ofori-Boateng et al. [9, 17]
		77.05%	Castiñeiras-Filho et al. [32]
Distillation column	Stages 11 N° min. stages 5	Stages 8	Ofori-Boateng et al. [9, 17]

Ofori-Boateng et al. [9] presented eight ideal stages, one condenser, a reflux ratio of 1.5, and an exergy destruction of 808 MJ. The low reflux ratio resulted in an almost horizontal rectifying line, and the feed flow should be cooled to reach the minimum reflux ratio. There is no explanation for these data in Ofori-Boateng et al. [9]. The distillation of Palacios-Bereche et al. [34] reached a similar exergy efficiency value (94%). The authors separated ethanol and water for ethanol production.

Glycerin is separated from water by flash distillation at a low pressure of 10 mmHg abs (1.33 kPa). An expansion valve reduces the temperature from 99.52 to 11.74 °C. Heat exchanger #5 is driven by 1360 kg of steam (100 °C), heats the mixed flow to 63 °C, and separates water and glycerin. The flash separator destroys 499.34 MJ of exergy, with a 78.82% efficiency. The exergy efficiency obtained herein for the column distillation is similar to Osuolale et al. [35], who obtained efficiencies between 68.8 and 79% for the water–methanol distillation process. The hydro-cyclone separates the catalyst from glycerin, destroying 18.89 MJ of exergy with an exergy efficiency of 98%. No data were reported for the hydro-cyclone in Ofori-Boateng et al. [9].

The global exergy efficiency obtained in this work is 17.07%, which is mainly due to the exergy destruction in the PBR. Ofori-Boateng et al. [9] obtained an overall exergy efficiency of 36%, and the pieces of equipment that destroyed the most exergy were centrifuge #1 (925 MJ) and dryer #2 (887 MJ). The global exergy efficiency of Castiñeiras-Filho and Pradelle [32] was 28.97%. The lower global exergy efficiency obtained herein is due to the lower cultivation efficiency in the PBR raceway (11.46%), against 99.47% of [36].

Comparison of results with existing studies is somewhat hindered because most focus on applications of biodiesel within internal combustion engines, evaluating blends and emissions. Few studies actually focus on the production process itself, with wide variation in the results obtained. As presented herein, some results are similar, of the same magnitude. When a high divergence was found, we attempted to reproduce the original results with the data included in the studies (when available). Although we have employed a different microalgae characterization model, we were able to track the repercussions of this choice in the results. However, for other parameters, this was not possible, leading to confirmation of inconsistencies, which could ultimately unfortunately result in the drawing of erroneous conclusions.

Exergy analysis had already been suggested by Talens et al. [36] as an environmental assessment tool for the comparison of energy sources and processes/routes in biodiesel production, being an important tool to help formulate adequate policies directed to the use of resources. Peralta-Ruiz et al. [37] employed exergy analysis to help design the biodiesel and bioethanol production process from microalgae, obtaining an overall exergy efficiency of 88.6%. The authors highlighted that economic and environmental evaluations should follow their study to provide a broader perspective on the conclusions.

More recently, Khoobbakht et al. [38] conducted an exergy assessment of transesterification in biodiesel production from

waste cooking canola oil. The authors obtained 91.7% exergy efficiency at 55 °C reaction temperature. It was verified that the excessive use of methanol and catalyst reduced the yield of biodiesel and that the exergy efficiency decreased as exergy losses increased by waste materials. Focusing on microalgae biodiesel, Gozmen Sanli et al. [39] evaluated the thermodynamic performance of an internal combustion engine using microalgae biodiesel. The energy input and exergy converted into useful work were slightly higher for conventional diesel fuel than for microalgae biodiesel. However, the thermoeconomic assessment revealed that energy and exergy losses per capital cost were lower for microalgae biodiesel. Ojeda et al. [40] mentioned that exergy analysis can compare microalgae-to-product pathways and establish which products and technologies are more suitable. The authors carried out the exergy assessment of biodiesel production from *Chlorella vulgaris* microalgae through acid esterification and basic transesterification using methanol and compared it with a process using pretreatment with $ZnCl_2$ and basic transesterification with ethanol. Considering industrial biodiesel production, the former is recommended as it presented an exergy efficiency of 82% against 50% for the pretreatment case.

However, even exergy assessments have limits for system improvement. As mentioned by Babaie [41], there are limiting factors for system performance that cannot be changed. Nevertheless, there are margins for improvement of efficiency when, for example, the minimum exergy required for the algal production process is identified and compared with the actual exergy consumed [42].

The main differences between our results and literature data are summarized in Table 6, which shows a comparison of the algae concentrations, increase in produced biomass, specific physical exergies, exergy efficiencies, and distillation column.

Finally, exergy analysis can provide the degree of sustainability of a biodiesel production process, with information on irreversibilities and losses. Microalgae biodiesel can contribute to achieving Sustainable Development Goal (SDG) 13 (climate action) and SDG 7 (affordable and clean energy), becoming promising alternatives to increase sustainable development in this sector. After pinpointing the sources of exergy-related inefficiencies within the microalgae biodiesel production, solutions and strategies can be recommended.

Conclusions

This study presented a detailed exergy analysis of microalgae biodiesel production, encompassing algae cultivation, oil extraction, transesterification, biodiesel separation, and methanol recovery. The products are biodiesel and glycerin. The lowest energy efficiency is obtained at the photobioreactor raceway due to its high exergy destruction. The exergy efficiency of the oil extraction process is higher than other studies due to the algae characterization model employed herein. This study critically compared the results obtained with scientific literature data, highlighting data gaps and inconsistencies. Further research should be carried out for another cycle of biodiesel production to compare the components and phases' efficiencies.

Funding The authors wish to acknowledge the financial support of the Brazilian National Council for Scientific and Technological Development (CNPq) for the MSc. scholarship and productivity grant 309452/2021–0.

Data Availability All availabile data is included into Results and Discussions section.

References

1. Ritchie H, Roser M, Rosado P(2022) - Energy. Our world in data. https://ourworldindata.org/energy. Accessed 12 Jan 2023
2. Caliskan H (2017) Environmental and enviroeconomic researches on diesel engines with diesel and biodiesel fuels. J Clean Prod 154:125–129. https://doi.org/10.1016/j.jclepro.2017.03.168
3. da Silva CA, Conejero MA, Barros Ribeiro EC, Batalha MO (2019) Competitiveness analysis of "social soybeans" in biodiesel production in Brazil. Renew Energy 133:1147–1157. https://doi.org/10.1016/j.renene.2018.08.108
4. Costa MW, Oliveira AAM (2022) Social life cycle assessment of feedstocks for biodiesel production in Brazil. Renew Sustain Energy Rev. https://doi.org/10.1016/j.rser.2022.112166
5. Grangeia C, Santos L, Lazaro LLB (2022) The Brazilian biofuel policy (RenovaBio) and its uncertainties: an assessment of technical, socioeconomic and institutional aspects. Energy Convers Manag: X https://doi.org/10.1016/j.ecmx.2021.100156
6. Kumar SC, Thakur AK, Aseer JR (2022) Algae biofuel as a substitute for compression ignition engine: a review. In: Verma P, Samuel OD, Verma TN, Dwivedi G (ed) Advancement in materials, manufacturing and energy engineering, Vol. I. Lecture Notes in Mechanical Engineering. Springer, Singapore. 43–51
7. Ketheesan B, Nirmalakhandan N (2012) Feasibility of microalgal cultivation in a pilot-scale airlift-driven raceway reactor. Bioresour Technol 108:196–202. https://doi.org/10.1016/j.biortech.2011.12.146
8. Bejan A, Tsatsaronis G, Moran M (1996) Thermal design & optimization. John Wiley & Sons, New York
9. Ofori-Boateng C, Lee KT, Lim J (2012) Sustainability assessment of microalgal biodiesel production processes: an exergetic analysis approach with Aspen Plus. Int J Exergy. https://doi.org/10.1504/IJEX.2012.047510
10. Sorguven E, Özilgen M (2010) Thermodynamic assessment of algal biodiesel utilization. Renew Energy 35:1956–1966. https://doi.org/10.1016/j.renene.2010.01.024
11. Ryu HJ, Oh KK, Kim YS (2009) Optimization of the influential factors for the improvement of CO2 utilization efficiency and CO2 mass transfer rate. J Ind Eng Chem. https://doi.org/10.1016/j.jiec.2008.12.012
12. De Morais MG, Costa JAV (2007) Carbon dioxide fixation by *Chlorella kessleri*, *C. vulgaris*, *Scenedesmus obliquus* and *Spirulina* sp. cultivated in flasks and vertical tubular photobioreactors. Biotechnol Lett 29:1349–1352. https://doi.org/10.1007/s10529-007-9394-6

13. Mtaki K, Kyewalyanga MS, Mtolera MSP (2021) Supplementing wastewater with NPK fertilizer as a cheap source of nutrients in cultivating live food (*Chlorella vulgaris*). Ann Microbiol 71:7. https://doi.org/10.1186/s13213-020-01618-0
14. Mtaki K, Kyewalyanga MS, Mtolera MSP (2023) Replacing expensive synthetic media with banana stem compost extract medium for production of *Chlorella vulgaris*. Appl Phycol. https://doi.org/10.1080/26388081.2022.2140073
15. Chisti Y (2007) Biodiesel from microalgae. Biotechnol Adv. https://doi.org/10.1016/j.biotechadv.2007.02.001
16. Sorgüven E, Özilgen M (2013) Thermodynamic efficiency of synthesis, storage and breakdown of the high-energy metabolites by photosynthetic microalgae. Energy 58:679–687. https://doi.org/10.1016/j.energy.2013.06.003
17. Ofori-Boateng C, Keat TL, JitKang L (2012) Feasibility study of microalgal and jatropha biodiesel production plants: exergy analysis approach. Appl Therm Eng 36:141–151. https://doi.org/10.1016/j.applthermaleng.2011.12.010
18. Karami R, Hoseinpour M, Hassan NMS, et al (2022) Exergy, energy, and emissions analyses of binary and ternary blends of seed waste biodiesel of tomato, papaya, and apricot in a diesel engine. Energy Convers and Manag: X https://doi.org/10.1016/j.ecmx.2022.100288
19. Prasakti L, Pratama SH, Fauzi A et al (2020) Exergy analysis of conventional and hydrothermal liquefaction-esterification processes of microalgae for biodiesel production. Open Chem 18:874–881. https://doi.org/10.1515/chem-2020-0132
20. Lazzaretto A, Tsatsaronis G (2006) SPECO: a systematic and general methodology for calculating efficiencies and costs in thermal systems. Energy 31:1257–1289. https://doi.org/10.1016/j.energy.2005.03.011
21. Peralta-Ruiz Y, González-Delgado AD, Kafarov V (2013) Evaluation of alternatives for microalgae oil extraction based on exergy analysis. Appl Energy 101:226–236. https://doi.org/10.1016/j.apenergy.2012.06.065
22. F-chart software (2022) Engineering equation solver. https://fchartsoftware.com/ees/. Accessed 15 Jun 2023
23. Attarakih M, Fara DA, Sayed S (2001) Dynamic modeling of a packed-bed glycerol - water distillation column. Ind Eng Chem Res 40:4857–4865. https://doi.org/10.1021/ie000430y
24. Miao C, Chakraborty M, Chen S (2012) Impact of reaction conditions on the simultaneous production of polysaccharides and bio-oil from heterotrophically grown *Chlorella sorokiniana* by a unique sequential hydrothermal liquefaction process. Bioresour Technol 110:617–627. https://doi.org/10.1016/j.biortech.2012.01.047
25. Cavalcanti EJC, Ferreira JVM, Carvalho M (2021) Research on a solar hybrid trigeneration system based on exergy and exergoenvironmental assessments. Energies. https://doi.org/10.3390/en14227560
26. Wolframalpha (2022) Wolfram Alpha ChemicalData. In: Wolframalpha. https://www.wolframalpha.com. Accessed 20 Nov 2022
27. Sonntag R, Borgnakke C, van Wylen G (2003) Fundamentals of thermodynamics, 6th edn. John Wiley & Sons, New York
28. Ruscic B, Bross DH (2022) Active thermochemical tables. argone national laboratory. https://atct.anl.gov/Thermochemical%20Data/version%201.122/species/?species_number=1003. Accessed 13 Oct 2022
29. Barkan C, Deluca K, Preston M (2018) Design of a flexible, high-volume direct flue gas-to-algae conversion process for value-added bioproducts. Report, University of Pennsylvania. https://repository.upenn.edu/handle/20.500.14332/5923
30. Petela R (2003) Exergy of undiluted thermal radiation. Sol Energy. https://doi.org/10.1016/S0038-092X(03)00226-3
31. Cavalcanti EJC, Ferreira JVM, Carvalho M (2021) Exergy assessment of a solar-assisted combined cooling, heat and power system. Sustain Energy Technol Assess. https://doi.org/10.1016/j.seta.2021.101361
32. Castiñeiras-Filho SLP, Pradelle F (2023) Modeling of microalgal biodiesel production integrated to a sugarcane ethanol plant: energy and exergy efficiencies and environmental impacts due to trade-offs in the usage of bagasse in the Brazilian context. J Clean Prod 395:136461. https://doi.org/10.1016/j.jclepro.2023.136461
33. Kim H, Shin J, Lee D et al (2019) In situ solvent recovery by using hydrophobic/oleophilic filter during wet lipid extraction from microalgae. Bioprocess Biosyst Eng 42:1447–1455. https://doi.org/10.1007/s00449-019-02141-6
34. Palacios-Bereche R, Mosqueira-Salazar KJ, Modesto M et al (2013) Exergetic analysis of the integrated first- and second-generation ethanol production from sugarcane. Energy 62:46–61. https://doi.org/10.1016/j.energy.2013.05.010
35. Osuolale F, Zhang J (2015) Distillation control structure selection for energy-efficient operations. Chem Eng Technol 38:907–916. https://doi.org/10.1002/ceat.201400707
36. Talens L, Villalba G, Gabarrell X (2007) Exergy analysis applied to biodiesel production. Resour Conserv Recycl 51:397–407. https://doi.org/10.1016/j.resconrec.2006.10.008
37. Peralta-Ruiz Y, Obregon LG, González-Delgado Á (2018) Design of biodiesel and bioethanol production process from microalgae biomass using exergy analysis methodology. Chem Eng Trans 70:1045–1050. https://doi.org/10.3303/CET1870175
38. Khoobbakht G, Kheiralipour K, Rasouli H et al (2020) Experimental exergy analysis of transesterification in biodiesel production. Energy. https://doi.org/10.1016/j.energy.2020.117092
39. Gozmen Sanli B, Özcanli M, Serin H (2020) Assessment of thermodynamic performance of an IC engine using microalgae biodiesel at various ambient temperatures. Fuel. https://doi.org/10.1016/j.fuel.2020.118108
40. Ojeda KA, Sánchez-Tuirán E, Gonzalez-Diaz J et al (2020) Exergy analysis applied to microalgae-based processes and products. In: Maroneze MM, Queiroz MI, Zepka LQ (eds) Jacob-Lopes E. Handbook of microalgae-based processes and products, Academic Press, pp 841–859
41. Babaie M (2022) Exergy analysis of the third-generation biofuels. In: Jacob-Lopes E, Zepka LQ, Severo IA, Maroneze MM (eds) 3rd generation biofuels. Woodhead Publishing, pp 835–845
42. Beal CM, Hebner RE, Webber ME (2012) Thermodynamic analysis of algal biocrude production. Energy. https://doi.org/10.1016/j.energy.2012.05.003